

Dynamic characteristics analysis of partial-interaction composite continuous beams

Genshen Fang^{1a}, Jingquan Wang^{*2}, Shuai Li² and Shubin Zhang³

¹ State Key Laboratory for Disaster Reduction in Civil Engineering,
Tongji University, Shanghai 200092, P.R. China

² Key Laboratory of Concrete and Prestressed Concrete Structure of Ministry of Education,
School of Civil Engineering, Southeast University, Nanjing 210096, P.R. China

³ Jiangsu Province Communications Planning and Design Institute Co., Ltd., Nanjing 210005, P.R. China

(Received June 25, 2015, Revised February 29, 2016, Accepted March 07, 2016)

Abstract. The dynamic characteristics of continuous steel-concrete composite beams considering the effect of interlayer slip were investigated based on Euler Bernoulli's beam theory. A simplified calculation model was presented, in which the Mode Stiffness Matrix (MSM) was developed. The natural frequencies and modes of partial-interaction composite continuous beams can be calculated accurately and easily by the use of MSM. Proceeding from the present method, the natural frequencies of two-span steel-concrete composite continuous beams with different span-ratios (0.53, 0.73, 0.85, 1) and different shear connection stiffnesses on the interface are calculated. The influence pattern of interfacial stiffness on bending vibration frequency was found. With the decrease of shear connection stiffness on the interface, the flexural vibration frequencies decrease obviously. And the influence on low order modes is more obvious while the reduction degree of high order is more sizeable. The real natural frequencies of partial-interaction continuous beams commonly used could have a 20% to 40% reduction compared with the fully-interaction ones. Furthermore, the reduction-ratios of natural frequencies for different span-ratios two-span composite beams with uniform shear connection stiffnesses are totally the same. The span-ratio mainly impacts on the mode shape. Four kinds of shear connection stiffnesses of steel-concrete composite continuous beams are calculated and compared with the experimental data and the FEM results. The calculated results using the proposed method agree well with the experimental and FEM ones on the low order modes which mainly determine the vibration properties.

Keywords: partial-interaction; steel-concrete composite continuous beam; shear connection stiffness; mode stiffness matrix; dynamic analysis

1. Introduction

Steel-concrete composite continuous beams have superior economic performance compared with simply supported composite beams for higher span/depth ratios and less deflection etc. (Nie *et al.* 2009). The flexible shear connectors, such as headed studs are usually used to connect the steel beam and concrete slab. Owing to the influence of elastic shear connection between two

*Corresponding author, Associate Professor, E-mail: wangjingquan@seu.edu.cn

^a Ph.D. Candidate, E-mail: 2222tjfgs@tongji.edu.cn

components allowing them to slip relative to each other, so as to provide partial rather than full interaction. Furthermore, those composite structures can be subjected to different kinds of dynamic loadings, such as wind, earthquake, traffic and impact loadings. The vibration properties of partial-interaction composite continuous beams need to be explored with an applicable method.

Studies about dynamic characteristics of partial-interaction steel-concrete composite beams have been well established. The dynamic properties of simply supported composite beams with partial interaction were analyzed based on Euler-Bernoulli's beam theory (Girhammar and Pan 1993, Adam *et al.* 1997, Wu *et al.* 2007, Huang and Su 2008, Hou *et al.* 2012) and Timoshenko's beam theory (Berczynski and Wroblewski 2005, Xu and Wu 2007, Ranzi and Zona 2009, Nguyen *et al.* 2012). The experimental researches (Biscontin *et al.* 2000, Berczynski and Wroblewski 2010, Zhang 2014) and numerical analyses (Inoue and Ishikawa 2010, Wroblewski *et al.* 2012, Chakrabarti *et al.* 2013) were also carried out. All above researches show that the interlayer slip of partial-interaction composite beam results in the decrease of natural frequency. What is more, the lower degree of interlayer shear connection, the greater the extent of natural frequency decrease is. However, most of these studies were based on single span beams with different boundary conditions, such as simply supported, clamped and free. The researches about composite continuous beams are relatively few, especially on dynamic properties.

Traditional analysis procedure on the vibration of continuous beams by means of Dynamic Stiffness Matrix (DSM) and finite element method was widely used (Hayashikawa and Watanabe 1985). And the general dynamic three-moment equation was adopted commonly. However, all of these researches are applicable to continuous beams with equal spans or composite beams with full interaction. Qi *et al.* (2010) created three dynamic models by utilizing the principle of force balance and deformation compatibility condition based on Euler-Bernoulli's beam theory and Timoshenko's beam theory. It turned out that the natural frequency reduced obviously and the dynamic responses increased significantly when considering the effect of interlayer slip and shear deformation while there was no apparent influence on dynamic performance whether taking vertical uplift into account or not. Shen *et al.* (2011, 2012) investigated the dynamic behavior of partial-interaction composite beams by the state-space method. It presented the natural frequencies of two-span composite continuous beams in different axial force and boundary conditions. The results showed that axial compressive force would decrease the natural frequencies and vice versa. Zhou *et al.* (2013) derived the governing differential equation and a new method for analyzing the free vibration characteristics of steel-concrete continuous composite box girder, based on Hamilton principle, with consideration of the shear lag effect, slip, shear deformation and rotational inertia was proposed. Results indicated that the interlayer slip had great influence on the natural frequency of the steel-concrete continuous composite box girder. As a result, it is essential to propose an applicable method which can be used to investigate the effects of interlayer slip on the dynamic characteristics of composite continuous beams definitely.

In the present study, a new method, which utilized the Euler-Bernoulli's beam theory, was presented to analyze the dynamic characteristics of partial-interaction composite continuous beams. It created a new model in which the mid-supports of continuous beam would be equivalent to the forced loads. And formulas for calculating the natural frequencies of composite continuous beam were derived. On the basis of the presented formulas, calculation and analyses on the dynamic characteristics of equal-span and unequal-span composite continuous beams were carried out. Besides, one dimensional finite element numerical simulations were made to verify the theoretical results. Clearer cognition about dynamic characteristics of partial-interaction composite continuous beams was gained through these researches.

2. Basic analysis model and calculation theory

Referring to the previous researches, the governing differential equations of motion for composite beams have been derived based on Euler-Bernoulli's beam theory (Girhammar and Pan 1993, Adam *et al.* 1997, Wu *et al.* 2007, Huang and Su 2008, Hou *et al.* 2012). The exact dynamic analysis procedure in the next section will be based on their research results. And this section will give a brief introduction. Fig. 1 shows the steel-concrete composite beam model and its cross section parameters. The x -axis is the neutral axis of the full-interaction composite beam. E_i , I_i , A_i and m_i ($i = 1, 2$) denote the Young's modulus, area moment of inertia, cross-sectional area and the mass of the composite beam per unit length, respectively. L is the length of the beam and the symbols h , h_1 , h_2 , and y_2 , standing for a few distances, are plotted in Fig. 1. And $h = h_1 + h_2$ signifies the distance of centroid of concrete slab to the centroid of steel beam. The support conditions are not specified, since they can be any kinds.

There are four assumptions used in this mechanical model.

- (1) The model is based on Euler-Bernoulli's beam theory which means the shear deformation and rotary inertia will not be considered and plane cross-section assumption is applied to concrete slab and steel beam. This assumption can be met since the height-to-length aspect ratio of steel-concrete composite beam is usually not very large and Xu and Wu (2007) have found that the shear deformation and rotary inertia made little difference on low order modes.
- (2) All the constitutive materials behave linearly and the deformations are small. The horizontal shear on the contact interface is proportional to the relative slip.
- (3) No transverse separation occurs on the contact interface of steel-concrete composite beam, therefore the steel beam and concrete slab meet the vertical deformation compatibility condition. Qi *et al.* (2010) found out that there was no apparent influence on dynamic performance whether taking vertical uplift into account or not.
- (4) The shear connectors between steel beam and concrete slab are continuous and uniformly distributed longitudinally which signifies the horizontal shear on the contact interface uniformly distributed longitudinally. Also the initial cohesive force and damping are neglected.

Considering the free-body diagram of a differential element in the composite beam subject to transverse load as shown in Fig. 2. Moment, shear force, normal force and slip force per unit length are denoted as M , V , N and Q_s , respectively.

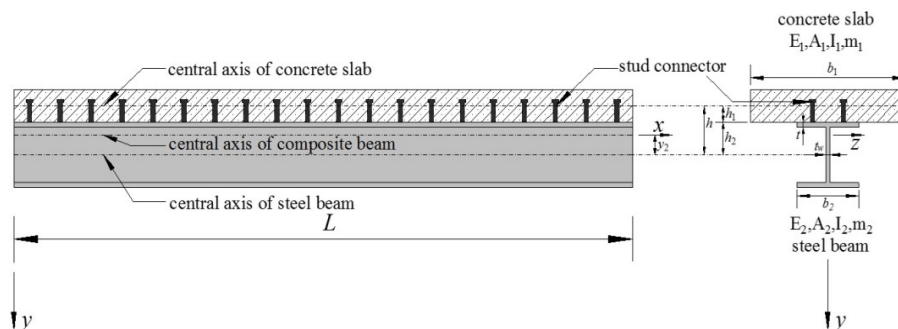


Fig. 1 Geometric parameters of steel-concrete composite beam and the coordinate system

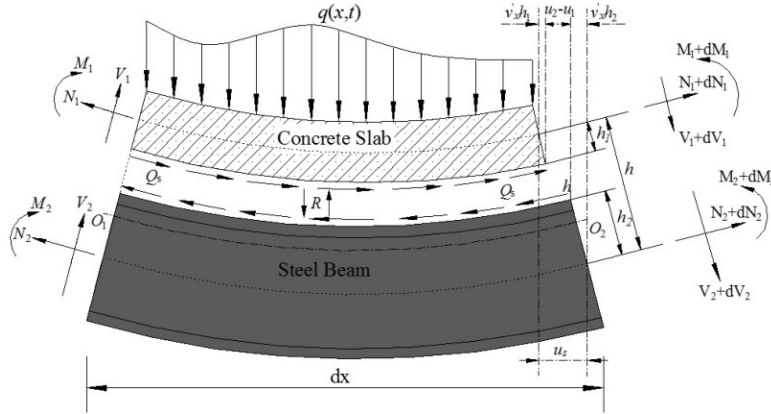


Fig. 2 Differential element in the composite beam subject to a distributed transverse load

A differential equation in terms of the displacement $v(x,t)$ is derived based on the above assumptions (in the case of no axial force).

$$\beta^2 \tilde{E}I \frac{\partial^6 v(x,t)}{\partial x^6} - \alpha^2 \tilde{E}I \frac{\partial^4 v(x,t)}{\partial x^4} + m \frac{\partial^4 v(x,t)}{\partial x^2 \partial t^2} - m \alpha^2 \frac{\partial^2 v(x,t)}{\partial t^2} = -\alpha^2 q(x,t) + \frac{\partial^2 q(x,t)}{\partial x^2} \quad (1)$$

where

$$\tilde{E}I = E_1 I_1 + E_2 I_2 + \frac{E_1 A_1 E_2 A_2}{E_1 A_1 + E_2 A_2} h^2, \quad \alpha^2 = k_s \left(\frac{1}{E_1 A_1} + \frac{1}{E_2 A_2} \right), \quad \beta^2 = \frac{\sum EI}{\tilde{E}I}$$

$\tilde{E}I$ is the equivalent flexural stiffness of the composite beam when the stiffness of the shear connector approaches infinity which means the full-interaction composite beam. Factor α^2 varies with the shear connection degree, which represents the relative relationship between longitudinal shear stiffness and axial stiffness of components per unit length. Factor β^2 indicates the flexural stiffness of the full-interaction composite beam increases $1/\beta^2$ times compared to the non-interaction composite beam.

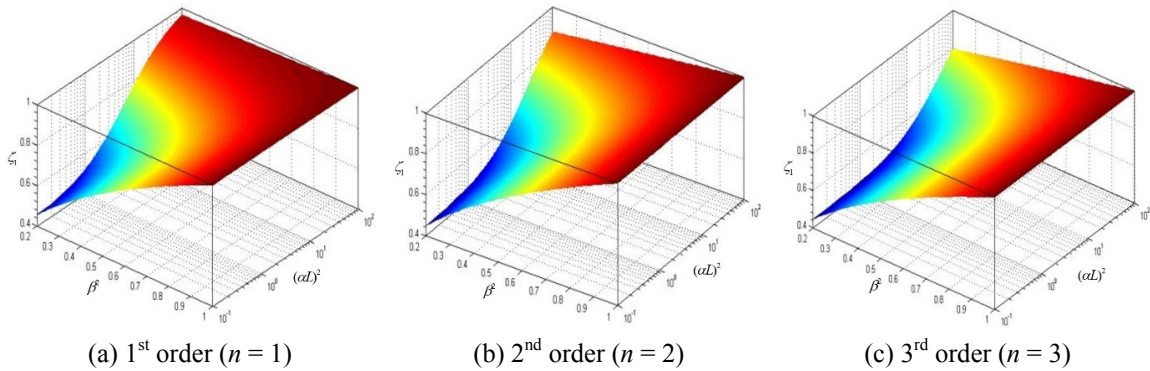


Fig. 3 Relationships of $\zeta_n - \beta^2$ and $\zeta_n - (\alpha L)^2$

Taking into consideration of the simply supported boundary conditions, the formula for calculating the natural frequencies of partial interaction composite beam can be expressed as

$$\omega_n = \zeta_n \tilde{\omega}_n \tag{2}$$

where subscript n denotes the n -th order mode of composite beam. And ζ_n is a reduction factor of n -th order natural frequency of partial-interaction composite beams relative to full-interaction ones which are represented by $\tilde{\omega}_n$. They are defined as

$$\zeta_n = \sqrt{\frac{\beta^2 + (\alpha L / n\pi)^2}{1 + (\alpha L / n\pi)^2}} \tag{3}$$

$$\tilde{\omega}_n = \frac{(n\pi)^2}{L^2} \sqrt{\frac{\tilde{E}I}{m}} \tag{4}$$

Fig. 3 demonstrates the effects of the parameter β^2 and $(\alpha L)^2$ upon the reduction factor ζ_n . It is readily found that relationship of ζ_n and β^2 is a positive correlation. For a composite beam with uniform cross section and certain materials, parameter β^2 is a constant. The reduction factor ζ_n gradually tends to 1 with the increase of the parameter $(\alpha L)^2$. And it has a wider effect range on higher orders.

As a result, it can be known that the effect of connection degree on composite beams is significant. Especially, it directly influences the dynamic characteristics of composite beams. The reduction factor ζ_n varies with shear connection stiffness. All above analyses are based on simply supported beam. However, composite continuous beams are used more frequently in the actual projects. It is essential to have a clear understanding on the vibration properties of part-interaction composite continuous beams.

2.1 Natural vibration characteristics analysis

Fig. 4 shows the calculation model of continuous steel-concrete composite beam. The mid-supports are substituted equivalently for the forced loads $P_i(t)$. The origin of coordinates is at the first support and the coordinate value of the i -th mid-support is defined as x_i . ($i = 1, 2, 3 \dots N$, and N indicates the number of mid-supports). As a result, the vibration problem of continuous steel-

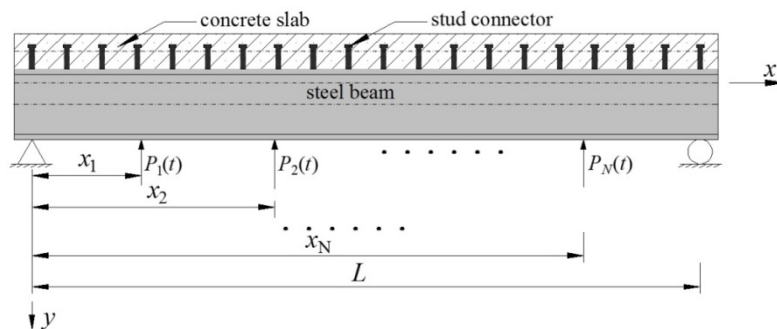


Fig. 4 The calculation model of continuous composite beam and the coordinate system

concrete composite beam is equivalent to the forced vibration problem of simply supported composite beam. And two conditions must be considered: (i) the boundary condition is same as the simply supported beam; (ii) the mid-supports meet the continuity condition including the continuity of force and deformation. Given that the varying patterns with time of constrained forces of mid-supports are same as the natural vibration of composite continuous beam. And the following formulas are satisfied.

$$v(x, t) = \Phi(x)e^{j\omega t} \quad (5)$$

$$v(x_i, t) = \Phi(x_i)e^{j\omega t} = 0 \quad (6)$$

$$q(x, t) = \sum_{i=1}^N P_i e^{j\omega t} \delta(x - x_i) \quad (7)$$

where j denotes the imaginary unit, ω denotes the circular frequency of vibration and $\delta(x - x_i)$ is a condition function defined as

$$\delta(x - x_i) = \begin{cases} 0, & x \neq x_i \\ 1, & x = x_i \end{cases} \quad (8)$$

Substituting Eqs. (5)-(7) into Eq. (1) yields

$$\begin{aligned} & \beta^2 \tilde{E}I \frac{\partial^6 \Phi(x)}{\partial x^6} - \tilde{E}I \alpha^2 \frac{\partial^4 \Phi(x)}{\partial x^4} + m\omega^2 \frac{\partial^2 \Phi(x)}{\partial x^2} - m\omega^2 \alpha^2 \Phi(x) \\ & = -\alpha^2 \sum_{i=1}^N P_i \delta(x - x_i) + \sum_{i=1}^N P_i \frac{\partial^2 \delta(x - x_i)}{\partial x^2} \end{aligned} \quad (9)$$

Introducing a parameter

$$t^2 = \frac{m\omega^2}{\tilde{E}I} \quad (10)$$

Making the Laplace transform of Eq. (9) produces

$$\begin{aligned} & (\beta^2 s^6 - \alpha^2 s^4 - t^2 s^2 + \alpha^2 t^2)L(\Phi) = (\beta^2 s^5 - \alpha^2 s^3 - t^2 s)\Phi(0) + (\beta^2 s^4 - \alpha^2 s^2 - t^2)\Phi^{(1)}(0) \\ & + (\beta^2 s^3 - \alpha^2 s)\Phi^{(2)}(0) + (\beta^2 s^2 - \alpha^2)\Phi^{(3)}(0) + \beta^2 s\Phi^{(4)}(0) + \beta^2 \Phi^{(5)}(0) + (s^2 - \alpha^2) \sum_{i=1}^N P_i e^{-sx_i} \end{aligned} \quad (11)$$

where the superscript (i) ($i = 1, 2, 3, 4, 5$) indicates the differential to coordinate x . Considering the boundary condition of simply supported beam and Eq. (11) can be simplified as

$$L(\Phi) = \frac{(\beta^2 s^4 - \alpha^2 s^2 - t^2)\Phi^{(1)}(0) + (\beta^2 s^2 - \alpha^2)\Phi^{(3)}(0) + \beta^2 \Phi^{(5)}(0) + (s^2 - \alpha^2) \sum_{i=1}^N P_i e^{-sx_i}}{\beta^2 s^6 - \alpha^2 s^4 - t^2 s^2 + \alpha^2 t^2} \quad (12)$$

Focusing on the formula as follow

$$\beta^2 s^6 - \alpha^2 s^4 - t^2 s^2 + \alpha^2 t^2 = 0 \tag{13}$$

Introducing a symbol $\Lambda = s^2$, Eq. (13) becomes

$$\beta^2 \Lambda^3 - \alpha^2 \Lambda^2 - t^2 \Lambda + \alpha^2 t^2 = 0 \tag{14}$$

It is a cubic equation of one variable. It can be shown that all three roots of Eq. (14) are real and one is negative while the other two are positive (see Appendix A in detail). Letting $\Lambda_1 < 0$, $\Lambda_2 > 0$, $\Lambda_3 > 0$ and they can be calculated as

$$\begin{aligned} \Lambda_1 &= \frac{\alpha^2 - 2\sqrt{\alpha^4 + 3t^2\beta^2} \cos \frac{\theta}{3}}{3\beta^2} \\ \Lambda_2 &= \frac{\alpha^2 + 2\sqrt{\alpha^4 + 3t^2\beta^2} \sin(\frac{\theta}{3} + \frac{\pi}{6})}{3\beta^2} \\ \Lambda_3 &= \frac{\alpha^2 + 2\sqrt{\alpha^4 + 3t^2\beta^2} \sin(\frac{\theta}{3} + \frac{5\pi}{6})}{3\beta^2} \end{aligned} \tag{15}$$

where

$$\theta = \arccos T \tag{16}$$

$$T = \frac{-2\alpha^6 - 9\alpha^2\beta^2t^2 + 27\alpha^2t^2\beta^4}{2\sqrt{(\alpha^4 + 3t^2\beta^2)^3}}, \quad (-1 < T < 1) \tag{17}$$

So the six roots of Eq. (13) are $s_{1,2} = \pm \lambda_1 j$, $s_{3,4} = \pm \lambda_2$, $s_{5,6} = \pm \lambda_3$, (j is the imaginary unit.), with

$$\pm \lambda_1 = \pm \sqrt{-\Lambda_1}, \quad \pm \lambda_2 = \pm \sqrt{\Lambda_2}, \quad \pm \lambda_3 = \pm \sqrt{\Lambda_3} \tag{18}$$

Then making the inverse Laplace transform of Eq. (12) produces

$$\begin{aligned} \Phi(x) &= c_1 \sin \lambda_1 x + c_2 \cos \lambda_1 x + c_3 \sinh \lambda_2 x + c_4 \cosh \lambda_2 x + c_5 \sinh \lambda_3 x + c_6 \cosh \lambda_3 x \\ &- \sum_{i=1}^N P_i \left[\frac{(\lambda_1^2 + \alpha^2) \sin \lambda_1 (x - x_i)}{\lambda_1 (\lambda_2^2 + \lambda_1^2)(\lambda_3^2 + \lambda_1^2)} + \frac{(\lambda_2^2 - \alpha^2) \sinh \lambda_2 (x - x_i)}{\lambda_2 (\lambda_1^2 + \lambda_2^2)(\lambda_3^2 - \lambda_2^2)} + \frac{(\lambda_3^2 - \alpha^2) \sinh \lambda_3 (x - x_i)}{\lambda_3 (\lambda_1^2 + \lambda_3^2)(\lambda_2^2 - \lambda_3^2)} \right] H(x - x_i) \end{aligned} \tag{19}$$

Where constants c_i ($i = 1, 2, 3, 4, 5, 6$) can be determined by the boundary conditions. And $H(x - x_i)$ is a condition function defined as

$$H(x - x_i) = \begin{cases} 0, & (x < x_i) \\ 1, & (x \geq x_i) \end{cases} \tag{20}$$

Taking into consideration of the boundary conditions of simply supported beam, c_i can be obtained (see Appendix B in detail)

$$c_2 = c_4 = c_6 = 0 \quad (21)$$

$$c_1 = \sum_{i=1}^N P_i \frac{(\lambda_1^2 + \alpha^2) \sin \lambda_1 (L - x_i)}{\lambda_1 (\lambda_2^2 + \lambda_1^2) (\lambda_3^2 + \lambda_1^2) \sin \lambda_1 L} \quad (22)$$

$$c_3 = \sum_{i=1}^N P_i \frac{(\lambda_2^2 - \alpha^2) \sinh \lambda_2 (L - x_i)}{\lambda_2 (\lambda_1^2 + \lambda_2^2) (\lambda_3^2 - \lambda_2^2) \sinh \lambda_2 L} \quad (23)$$

$$c_5 = \sum_{i=1}^N P_i \frac{(\lambda_3^2 - \alpha^2) \sinh \lambda_3 (L - x_i)}{\lambda_3 (\lambda_1^2 + \lambda_3^2) (\lambda_2^2 - \lambda_3^2) \sinh \lambda_3 L} \quad (24)$$

Substituting Eqs. (21)-(23) into Eq. (19), the mode shape function of composite continuous beam can be got

$$\begin{aligned} \Phi(x) = & \frac{(\lambda_1^2 + \alpha^2)}{\lambda_1 (\lambda_2^2 + \lambda_1^2) (\lambda_3^2 + \lambda_1^2)} \sum_{i=1}^N P_i \left[\frac{\sin \lambda_1 (L - x_i) \sin \lambda_1 x}{\sin \lambda_1 L} - \sin \lambda_1 (x - x_i) H(x - x_i) \right] \\ & + \frac{(\lambda_2^2 - \alpha^2)}{\lambda_2 (\lambda_1^2 + \lambda_2^2) (\lambda_3^2 - \lambda_2^2)} \sum_{i=1}^N P_i \left[\frac{\sinh \lambda_2 (L - x_i) \sinh \lambda_2 x}{\sinh \lambda_2 L} - \sinh \lambda_2 (x - x_i) H(x - x_i) \right] \\ & + \frac{(\lambda_3^2 - \alpha^2)}{\lambda_3 (\lambda_1^2 + \lambda_3^2) (\lambda_2^2 - \lambda_3^2)} \sum_{i=1}^N P_i \left[\frac{\sinh \lambda_3 (L - x_i) \sinh \lambda_3 x}{\sinh \lambda_3 L} - \sinh \lambda_3 (x - x_i) H(x - x_i) \right] \end{aligned} \quad (25)$$

Letting $x = x_k$ ($k = 1, 2, 3 \dots N$), and considering the deformation constraint conditions at each supports in Eq. (6). Eq. (25) becomes

$$\begin{aligned} \Phi(x_k) = & \frac{(\lambda_1^2 + \alpha^2)}{\lambda_1 (\lambda_2^2 + \lambda_1^2) (\lambda_3^2 + \lambda_1^2)} \sum_{i=1}^N P_i \left[\frac{\sin \lambda_1 (L - x_i) \sin \lambda_1 x_k}{\sin \lambda_1 L} - \sin \lambda_1 (x_k - x_i) H(x_k - x_i) \right] \\ & + \frac{(\lambda_2^2 - \alpha^2)}{\lambda_2 (\lambda_1^2 + \lambda_2^2) (\lambda_3^2 - \lambda_2^2)} \sum_{i=1}^N P_i \left[\frac{\sinh \lambda_2 (L - x_i) \sinh \lambda_2 x_k}{\sinh \lambda_2 L} - \sinh \lambda_2 (x_k - x_i) H(x_k - x_i) \right] \\ & + \frac{(\lambda_3^2 - \alpha^2)}{\lambda_3 (\lambda_1^2 + \lambda_3^2) (\lambda_2^2 - \lambda_3^2)} \sum_{i=1}^N P_i \left[\frac{\sinh \lambda_3 (L - x_i) \sinh \lambda_3 x_k}{\sinh \lambda_3 L} - \sinh \lambda_3 (x_k - x_i) H(x_k - x_i) \right] \end{aligned} \quad (26)$$

The Eq. (26) can be expressed as

$$\begin{bmatrix} A_{11} & A_{12} & \cdots & A_{1N} \\ A_{21} & A_{22} & \cdots & A_{2N} \\ \vdots & \vdots & \ddots & \vdots \\ A_{N1} & A_{N1} & \cdots & A_{NN} \end{bmatrix} \begin{Bmatrix} P_1 \\ P_2 \\ \vdots \\ P_N \end{Bmatrix} = 0 \quad \text{or} \quad \mathbf{AP} = \mathbf{0} \quad (27)$$

where

$$\begin{aligned}
 A_{ki} = & \frac{(\lambda_1^2 + \alpha^2)}{\lambda_1(\lambda_2^2 + \lambda_1^2)(\lambda_3^2 + \lambda_1^2)} \left[\frac{\sin \lambda_1(L - x_i) \sin \lambda_1 x_k}{\sin \lambda_1 L} - \sin \lambda_1(x_k - x_i)H(x_k - x_i) \right] \\
 & + \frac{(\lambda_2^2 - \alpha^2)}{\lambda_2(\lambda_1^2 + \lambda_2^2)(\lambda_3^2 - \lambda_2^2)} \left[\frac{\sinh \lambda_2(L - x_i) \sinh \lambda_2 x_k}{\sinh \lambda_2 L} - \sinh \lambda_2(x_k - x_i)H(x_k - x_i) \right] \\
 & + \frac{(\lambda_3^2 - \alpha^2)}{\lambda_3(\lambda_1^2 + \lambda_3^2)(\lambda_2^2 - \lambda_3^2)} \left[\frac{\sinh \lambda_3(L - x_i) \sinh \lambda_3 x_k}{\sinh \lambda_3 L} - \sinh \lambda_3(x_k - x_i)H(x_k - x_i) \right]
 \end{aligned} \tag{28}$$

For the full-interaction composite beam, A_{ki} can be expressed as

$$A_{ki} = \frac{\sin \lambda(L - x_i) \sin \lambda x_k}{\sin \lambda L} - \frac{\sinh \lambda(L - x_i) \sinh \lambda x_k}{\sinh \lambda L} + [\sinh \lambda(x_k - x_i) - \sin \lambda(x_k - x_i)]H(x_k - x_i) \tag{29}$$

where

$$\lambda = \sqrt{t} = \left(\frac{m\omega^2}{\tilde{EI}} \right)^{\frac{1}{4}} \tag{30}$$

And A_{ki} means the deformation value in the k -th support when i -th support under unit force. The matrix **A** is named “Mode Stiffness Matrix (MSM)” in this paper. It has following characteristic

$$A_{ki} = A_{ik} \tag{31}$$

The Eq. (31) can be proved easily by Eqs. (28)-(29). And it means MSM is a symmetric matrix. In the consideration of function $H(x - x_i)$ in Eq. (20), A_{ki} ($k \leq i$) can be simplified as

$$\begin{aligned}
 A_{ki} = & \frac{(\lambda_1^2 + \alpha^2)}{\lambda_1(\lambda_2^2 + \lambda_1^2)(\lambda_3^2 + \lambda_1^2)} \left[\frac{\sin \lambda_1(L - x_i) \sin \lambda_1 x_k}{\sin \lambda_1 L} \right] \\
 & + \frac{(\lambda_2^2 - \alpha^2)}{\lambda_2(\lambda_1^2 + \lambda_2^2)(\lambda_3^2 - \lambda_2^2)} \left[\frac{\sinh \lambda_2(L - x_i) \sinh \lambda_2 x_k}{\sinh \lambda_2 L} \right] \\
 & + \frac{(\lambda_3^2 - \alpha^2)}{\lambda_3(\lambda_1^2 + \lambda_3^2)(\lambda_2^2 - \lambda_3^2)} \left[\frac{\sinh \lambda_3(L - x_i) \sinh \lambda_3 x_k}{\sinh \lambda_3 L} \right]
 \end{aligned} \tag{32}$$

And for the full-interaction composite beam

$$A_{ki} = \frac{\sin \lambda(L - x_i) \sin \lambda x_k}{\sin \lambda L} - \frac{\sinh \lambda(L - x_i) \sinh \lambda x_k}{\sinh \lambda L} \tag{33}$$

Making a discussion of the Eq. (27):

- (1) When $P_i = 0$ ($i = 1, 2, 3 \dots N$), Eq. (27) is always true obviously, that is the antisymmetric modes of continuous composite beam with equal spans and uniform cross section. In this case, its vibration performance is equivalent to the simply supported composite beam, as shown in the Fig. 5.

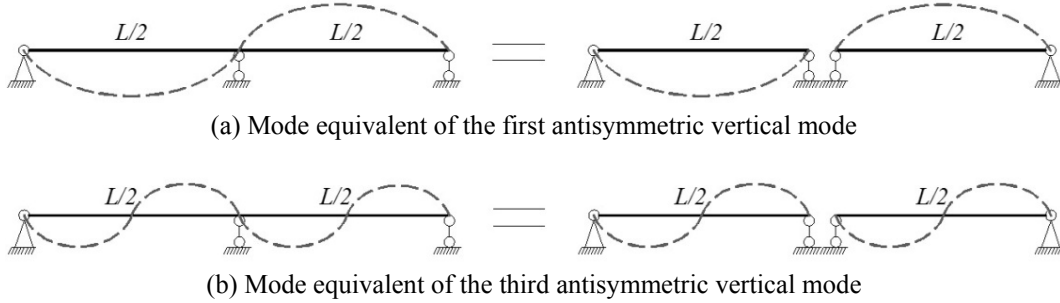


Fig. 5 Antisymmetric mode equivalent of continuous composite beam with equal spans and uniform cross section

As a result, the natural frequencies of composite continuous beam can be calculated by Eq. (2). And the L in Eq. (2) can be defined as the length of a single-span of composite continuous beam.

- (2) In another case, A non-trivial solution of the P_i , ($i = 1, 2, 3 \dots N$) can be obtained only when the determinant of the MSM vanishes. In this manner, the following frequency equation for composite continuous beam is determined

$$\begin{vmatrix} A_{11} & A_{12} & \cdots & A_{1N} \\ A_{21} & A_{22} & \cdots & A_{2N} \\ \vdots & \vdots & \ddots & \vdots \\ A_{N1} & A_{N1} & \cdots & A_{NN} \end{vmatrix} = 0 \quad \text{or} \quad |\mathbf{A}| = 0 \quad (34)$$

3. Application and discussion

In this section, numerical examples are presented for illustrating the proposed method and depicting the effect of shear connection stiffness of connectors upon the frequencies of the partial-interaction composite continuous beams. Fig. 6 shows the cross section of the beams. The shear stiffness of a single shear connector is determined by push-out test result (Zhang 2014). As shown in the Fig. 7, the total Q - s constitutive relationship of a stud in nonlinear. Johnson and May (1975) defined the tangent stiffness on the point of half ultimate capacity of studs as shear stiffness. Wang (1998) suggested the shear stiffness could be valued as tangent stiffness when slip was equal to 0.8 mm. Nie (2011) proposed a formula (Eq. (35)) to calculate the shear stiffness of a single shear connector based on a mass of experiments. Chinese specification GB 50017-2003, "Code for design of Steel structures" (2003), presented a method to calculate the shear stiffness of studs, as shown in Eq. (36).

$$K=0.66V_u \quad (35)$$

$$K=N_v^c \quad (36)$$

where V_u and N_v^c both denote the ultimate capacity a single shear connector.

According to above different methods, the values of shear connection stiffness for a single

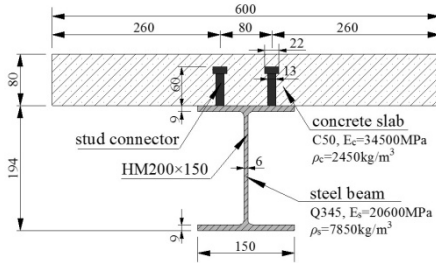


Fig. 6 Cross section of the continuous composite beam (mm)

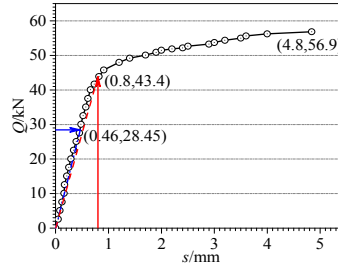


Fig. 7 Q-s constitutive relationship of a single stud

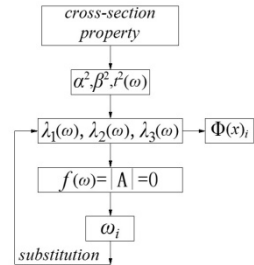


Fig. 8 Computation procedures

connector are 61.8 kN/mm (Johnson and May 1975), 54.3 kN/mm (Wang), 37.5 kN/mm (Nie), 56.9 kN/mm (Chinese specification GB 50017-2003), respectively. The first two results are approximate to the result obtained by Chinese specification GB 50017-2003. Therefore, the average of first two results is defined as the shear connection stiffness of a single connector in this paper. The value is 57.6 kN/mm.

The shear connection stiffness of the shear connector per unit length can be defined as

$$k_s = n_s K / p \tag{37}$$

where n_s , K , p denote the transversal rows of stud connectors, shear connection stiffness of a single connector, and longitudinal space, respectively. The composite continuous beams are divided into two kinds, one is with equal spans and the other is with unequal spans. And the mathematical software MATLAB is used to calculate the natural frequencies of the composite continuous beams. The computation procedures are showed in Fig. 8.

Due to the effect of computing time, two-span continuous beams with the different span-ratios are calculated. The span-ratios, 0.58 (2.8 m + 4.8 m), 0.73 (3.2 m + 4.4 m), 0.85 (3.5 m + 4.1 m), 1.00 (3.8 m + 3.8 m), are chosen. The shear connection stiffnesses of connectors per unit length k_s (N/mm²) are taken as 200 N/mm² to 1000 N/mm² at intervals of 100 N/mm². And four particular values, 311.4 N/mm², 384 N/mm², 500.9 N/mm², 768 N/mm², are also chosen in order to make a comparison with some experimental and computational results.

Fig. 9 shows the first six modes of two-span continuous beams. To illustrate the different span-ratios, four sub-labeled (a)-(d) are presented. They indicate the span-ratios, 0.58, 0.73, 0.85, 1.00, respectively. For the two-span continuous beams, with the decrease of span-ratio, the modes will change. Seen from the vibration energy perspective, it's a process of energy transmission. When span-ratio is small, the vibration of long span is excited more easily than the short span. As a result, the wave number of a certain mode on short span will decrease while it increases on long span with the reduction of span-ratio.

Fig. 10 shows that how the frequencies change in different shear connection stiffnesses (a) and the frequency reduction ratios of partial-interaction composite beams to fully-interaction ones (b). It turns out, however, that with the shear connection stiffness increasing, so does the frequency of composite continuous beam. And it changes closely in a linear trend with the increase of mode order. The natural frequencies of composite continuous beams with equal spans have several compact zones. It's same as the general continuous beams. And the other continuous beams with unequal spans are between each pair of compact zones. By comparison with the fully- interaction

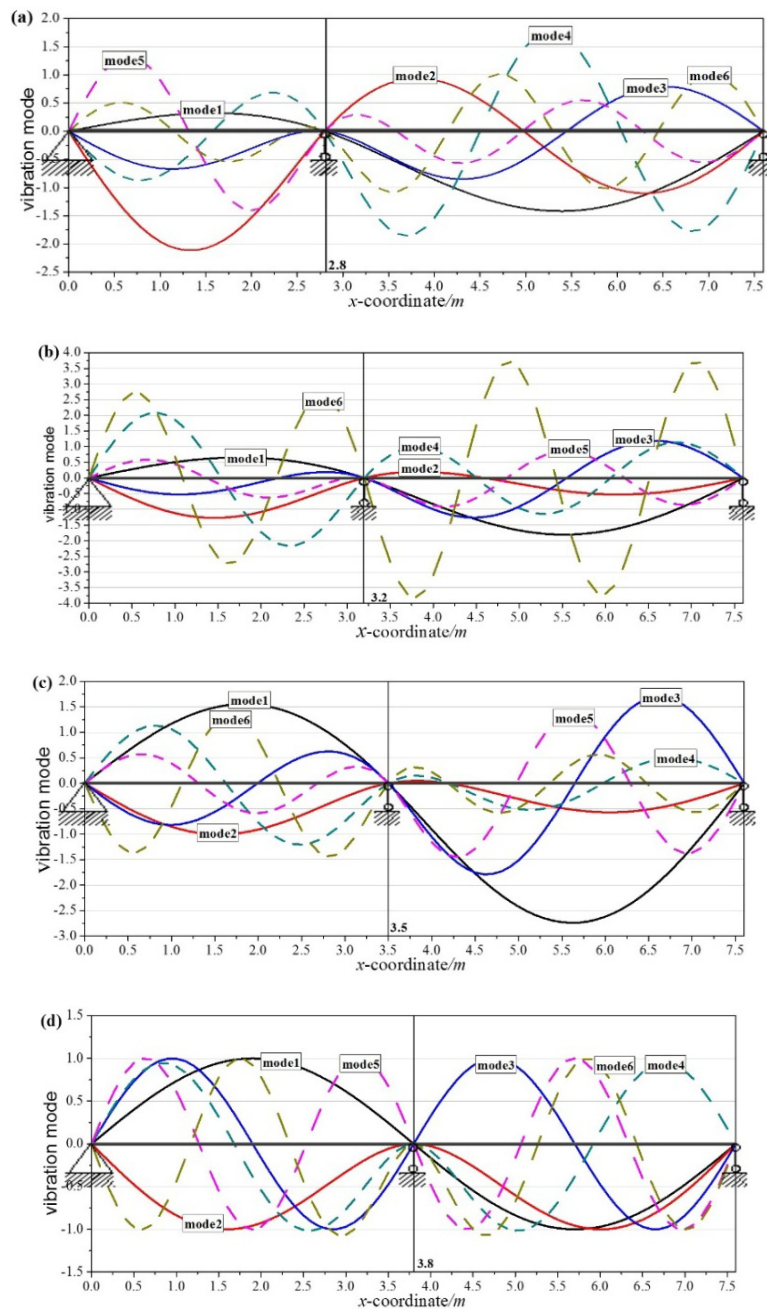


Fig. 9 First six modes of two-span continuous beams with different span-ratios

composite beams, the frequencies of partial-interaction ones get a reduction. That means the real natural frequencies of partial-interaction continuous beams commonly used could have a 20% to 40% reduction compared with the fully-interaction ones. Besides, the higher modes order, the higher reduction is. And span-ratios have little effect on the reduction of the natural frequencies.

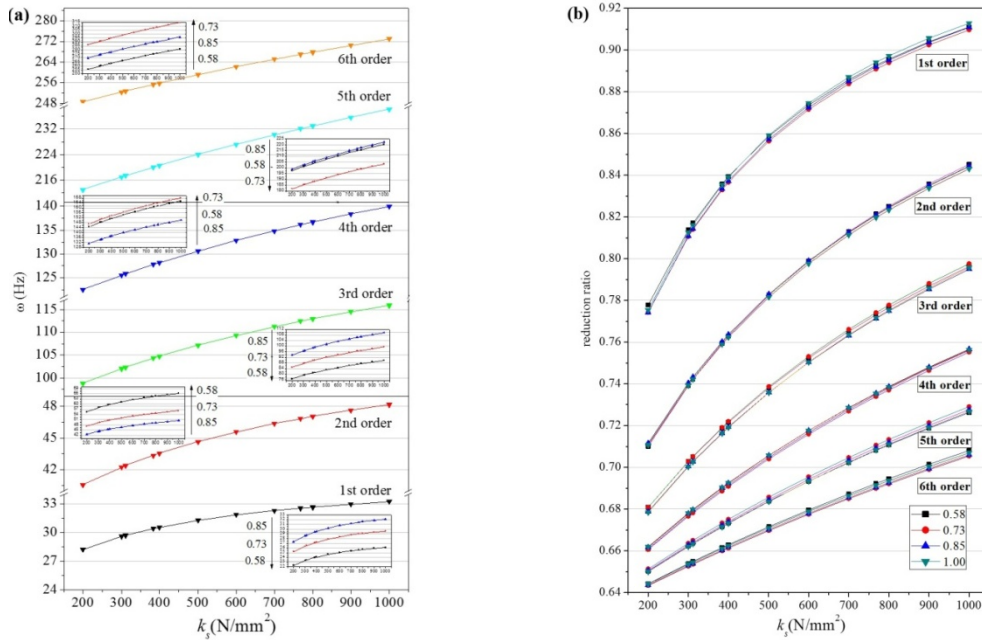


Fig. 10 Natural frequencies of two-span composite continuous beams with different span-ratios and shear connection stiffnesses

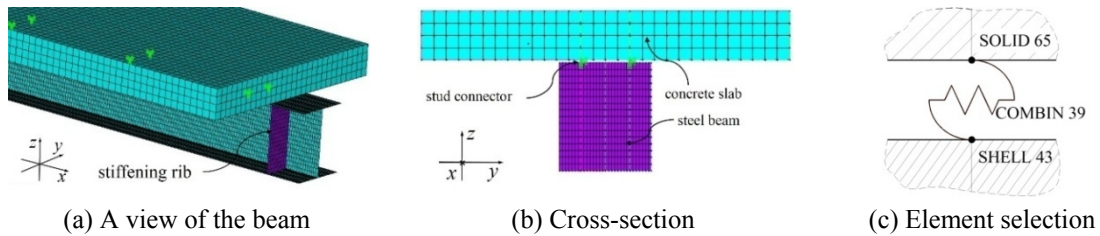


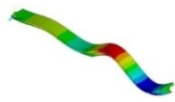
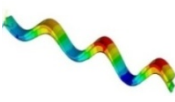
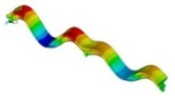
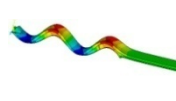
Fig. 11 The FE model of the steel-concrete composite beam

4. Verification of numerical analysis results

This section will give the experimental results and computational results based on FE software ANSYS to verify the theoretical and numerical results. And the experimental results refer to Zhang (2014) which carried out four ordinary steel-concrete composite beams (CB1~CB4) with the different shear connection stiffness on the interlayer. The values of k_s (N/mm²) are 311.4, 384.0, 500.9, 768.0, respectively.

The finite element model is established for the continuous composite beams, as shown in Fig. 10. The concrete slab and steel beam are modeled, respectively, with elements SOLID 65 and SHELL 43. The nonlinear spring element COMBIN39 is selected to simulate the stud connector. And the conjunction nodes between concrete slab and steel beam are coupled on the vertical and transverse direction, but not on the longitudinal direction. The shear connection stiffness of a single connector is 57.6 kN/mm. Applying the same parameters showed in Fig. 6 to the FE model,

Table 1 Natural frequencies and modes of composite continuous beams (vertical bending vibration)

Mode order	K_s / N/mm	(3.8 m + 3.8 m)			(4.8 m + 2.8 m)			
		Mode shape and frequencies by FEM/Hz	Theoretical results/Hz	Experimental results/Hz	Mode shape and frequencies by FEM/Hz	Theoretical results/Hz		
The 1 st	311.4		30.20	29.72	28.74		23.46	23.43
	384.0		30.49	30.42	29.99		23.68	23.97
	500.9		30.71	31.29	31.25		23.88	24.63
	768.0		31.07	32.56	32.52		24.16	25.60
The 2 nd	311.4		41.69	42.39	—		58.38	58.17
	384.0		42.58	43.35	—		59.31	59.52
	500.9		42.90	44.65	—		60.0	61.33
	768.0		43.79	46.82	—		61.32	64.38
The 3 rd	311.4		105.93	102.33	97.18		71.63	79.35
	384.0		108.65	104.33	99.54		72.78	80.89
	500.9		109.95	107.19	102.52		73.80	83.07
	768.0		113.32	112.41	109.90		75.50	87.01
The 4 th	311.4		120.26	125.84	—		140.56	148.59
	384.0		123.95	127.79	—		143.70	150.90
	500.9		124.80	130.65	—		146.87	154.30
	768.0		128.50	136.11	—		152.03	160.86
The 5 th	311.4		185.85	217.40	194.13		163.90	201.32
	384.0		191.35	220.04	198.07		168.34	203.77
	500.9		194.57	224.05	201.37		170.92	207.46
	768.0		202.76	232.14	205.41		177.87	214.86
The 6 th	311.4		190.02	252.79	—		201.05	260.15
	384.0		199.15	255.30	—		206.85	262.78
	500.9		202.40	259.12	—		211.24	266.78
	768.0		209.30	266.98	—		220.07	274.99

the natural frequencies and mode shapes are computed, as described in Table 1.

Tables 1-3 show the results and ratios of computational and experimental data of first six vertical bending vibration frequencies. As presented in Tables 1-2, theoretical results are little higher than the experimental results. And it shows the results calculated by proposed method agree well with the experimental results, with mean $f^{\text{MSM}} / F^{\text{EXP}}$ values of below 1.12, and standard deviation values of below 0.016. Besides, the difference shows almost no change with the increase of shear connection stiffness. However, it shows a rising trend with the increase of mode orders, i.e., the mean value increases from 1.01 to 1.12. It is closely related to the local distortion since MSM is based on the Euler-Bernoulli beam theory. The stiffness of composite beam based on the proposed theoretical model will be little higher than the actual structure. Besides, the shear connector and natural cohesive action between concrete slab and steel beam are not completely equivalent to the uniformly distributed shear force.

Table 2 MSM method versus experiment and FEM results of first six natural frequencies (3.8 m + 3.8 m)

$K_s/$ N/mm	$f_{i_{VB}}^{MSM} / f_{i_{VB}}^{EXP} *$			$f_{i_{VB}}^{MSM} / f_{i_{VB}}^{FEM} *$					
	1 st order	3 rd order	5 th order	1 st order	2 nd order	3 rd order	4 th order	5 th order	6 th order
311.4	1.03	1.05	1.12	0.98	1.02	0.97	1.05	1.17	1.33
384.0	1.01	1.05	1.11	1.00	1.02	0.96	1.03	1.15	1.28
500.9	1.00	1.05	1.11	1.02	1.04	0.97	1.05	1.15	1.28
768.0	1.00	1.02	1.13	1.05	1.07	0.99	1.06	1.14	1.28
Mean	1.01	1.04	1.12	1.01	1.04	0.97	1.05	1.15	1.29
Standard deviation	0.016	0.013	0.009	0.028	0.025	0.014	0.012	0.011	0.026

* $f_{i_{VB}}^{MSM} / f_{i_{VB}}^{EXP}$ and $f_{i_{VB}}^{MSM} / f_{i_{VB}}^{FEM}$: $f_{i_{VB}}^{MSM}$, $f_{i_{VB}}^{EXP}$, $f_{i_{VB}}^{FEM}$ denote the natural frequency of i -th vertical bending vibration mode gained by presented theoretical method based MSM, experiment and FEM, respectively (similarly hereinafter)

Table 3 MSM method versus FEM results of first six natural frequencies (4.8 m + 2.8 m)

$K_s/$ N/mm	$f_{i_{VB}}^{MSM} / f_{i_{VB}}^{FEM} *$					
	1 st order	2 nd order	3 rd order	4 th order	5 th order	6 th order
311.4	1.00	1.00	1.11	1.06	1.23	1.29
384.0	1.01	1.00	1.11	1.05	1.21	1.27
500.9	1.03	1.02	1.13	1.05	1.21	1.26
768.0	1.06	1.05	1.15	1.06	1.21	1.25
Mean	1.03	1.02	1.12	1.05	1.22	1.27
Standard deviation	0.026	0.024	0.020	0.004	0.009	0.019

As can be seen in Tables 1 and 3, the first six vertical bending frequencies calculated by the MSM and FEM are compared. The comparisons show good agreement between the experimental and predicted frequencies, with mean $f_{i_{VB}}^{MSM} / f_{i_{VB}}^{FEM}$ values of below 1.29 (3.8 m + 3.8 m) and 1.27 (4.8 m + 2.8 m), and standard deviation values of below 0.028 and 0.026, respectively. Similarly, the shear connection stiffness has little effects on the difference of the same order. Overall, it shows a rising trend with the increase of mode orders. The solid and shell element used on FE analysis could generate local deformation. The spring element is also not really match the real stud connector. So, the relative deviations between the theoretical results and FEM results are inevitable.

Although the relative deviations get larger with the increase of order, in actual practice, the low order modes are focused on more since the vibration properties of composite beam are determined by them to great extent. The mean frequency ratios of the first four orders are below 1.05 (equal spans) and 1.12 (unequal spans). Consequently, the results gained by present calculation method based on MSM are consistent with the experimental and FEM results well as a whole. And it meet the needs of practical engineering.

5. Conclusions

On the strength of previous researches, a “Model Stiffness Matrix (MSM)” was obtained from an exact analysis procedure based on the one-dimensional linear elastic partial-composite action theory. The natural frequencies and modes of composite continuous beams can be calculated accurately by the MSM with the help of mathematical software. The proposed method is general in nature and can be applied to different span arrangement, material and geometry parameters. And an exact analysis of natural vibration properties of composite continuous beams with different span-ratios and shear connection stiffnesses on the interface was carried out by use of the present method. The previous experimental and finite element results were compared to verify the theoretical results. Several main conclusions that can be drawn from above investigations:

- The natural frequencies of composite continuous beam increase in a linear trend along with the shear connection stiffnesses on the interface. The natural frequencies of composite continuous beams with equal spans have several compact zones. It's same as the general continuous beams. And natural frequencies of the other continuous beams with non-equal spans are between each pair of compact zones.
- It's obviously that the frequencies of partial-interaction composite continuous beams get a reduction compare with the fully-interaction ones. And the real natural frequencies of partial-interaction composite continuous beams commonly used could have a 20% to 40% reduction. The higher order and the lower shear connection stiffness, the higher reduction. Meanwhile, the reduction ratio is in the inverse proportional relationship to the shear stiffness of connectors. And its magnitude of higher order modes is bigger. The higher order, the smoother variation trend is. In addition, span-ratio has little effects on the reduction of the natural frequencies.
- With respect to the natural frequencies of low order modes which mainly determine the vibration properties, the results conduct by experiments and FEM agree well with the results gained by present theoretical method based on MSM. In other words, the present method has enough precision and meet the needs of practical engineering.

As a result, the reduction of natural frequencies for partial-interaction composite continuous beams cannot be ignored. And the proposed method will help a lot to make the dynamic analyses of composite continuous beams.

In the analysis, however, the influence of shear deformation, rotary inertia and other nonlinear factors was not considered, and the MSM was derived from the specific boundary condition which was simply supported and with uniform section. It's worth mentioning that further research on those aspects is in the works.

Acknowledgments

The research described in this paper was financially supported by National Science and Technology Support Program, China (Grant No. 2011BAJ09B02), Six talent peaks project in Jiangsu Province (Grant No. JZ-007), and the Fundamental Research Funds for the Central Universities. The financial supports are greatly appreciated.

References

- Adam, C., Heuer, R. and Jeschko, A. (1997), "Flexural vibrations of elastic composite beams with interlayer slip", *Acta. Mech.*, **125**(1-4), 17-30.
- Berczynski, S. and Wroblewski, T. (2005), "Vibration of steel-concrete composite beams using the Timoshenko beam mode", *J. Vib. Control*, **11**(6), 829-848.
- Berczynski, S. and Wroblewski, T. (2010), "Experimental verification of natural vibration models of steel-concrete composite beams", *J. Vib. Control*, **16**(14), 2057-2081.
- Biscontin, G., Morassi, A. and Wendel, P. (2000), "Vibrations of steel-concrete composite beams", *J. Vib. Control*, **6**(5), 691-714.
- Chakrabarti, A., Sheikh, A.H., Griffith, M. and Oehlers, D.J. (2013), "Dynamic response of composite beams with partial shear interaction using a higher-order beam theory", *J. Struct. Eng.*, **139**(1), 47-56.
- Girhammar, U.A. and Pan, D.H. (1993), "Dynamic analysis of composite members with interlayer slip", *Int. J. Solids. Struct.*, **30**(6), 797-823.
- Hayashikawa, T. and Watanabe, N. (1985), "Free vibration analysis of continuous beams", *J. Eng. Mech.*, **111**(5), 639-652.
- Hou, Z.M., Xia, H. and Zhang, Y.L. (2012), "Dynamic analysis and shear connector damage identification of steel-concrete composite beams", *Steel Compos. Struct., Int. J.*, **13**(4), 327-341.
- Huang, C.W. and Su, Y.H. (2008), "Dynamic characteristics of partial composite beams", *Int. J. Struct. Stab. Dy.*, **8**(4), 665-685.
- Inoue, K. and Ishikawa, K. (2010), "Free vibration analysis of multi layered beam members including the effect of interlayer slip", *Int. J. Struct. Eng.*, **1**(3/4), 327-339.
- Johnson, R.P. and May, I.M. (1975), "Partial-interaction design of composite beams", *Struct. Eng.*, **53**(8), 305-311.
- Nguyen, Q.H., Hjiatj, M. and Grogneq, P.L. (2012), "Analytical approach for free vibration analysis of two-layer Timoshenko beams with interlayer slip", *J. Sound. Vib.*, **331**(12), 2949-2961.
- Nie, J.G. (2011), *Steel-Concrete Composite Bridges*, China Communications Press, Beijing, China. [In Chinese]
- Nie, J.G., Tao, M.X., Cai, C.S. and Li, S.J. (2009), "Deformation analysis of prestressed continuous steel-concrete composite beams", *J. Struct. Eng.*, **135**(11), 1377-1389.
- Qi, J.J., Jiang, L.Z., Zhang, C.Z. and Yu, Z.W. (2010), "Effects of interface slip, vertical uplift and shear deformation on dynamic behavior of steel-concrete composite continuous beams", *J. Central South Univ. (Science and Technology)*, **41**(6), 2334-2343. [In Chinese]
- Ranzi, G. and Zona, A. (2009), "A steel-concrete composite beam model with partial interaction including the shear deformability of the steel component", *Eng. Struct.*, **29**(11), 3026-3041.
- Shen, X.D., Chen, W.Q., Wu, Y.F. and Xu, R.Q. (2011), "Dynamic analysis of partial-interaction composite beams", *Compos. Sci. Technol.*, **71**(10), 1286-1294.
- Shen, X.D., Chen, W.Q. and Xu, R.Q. (2012), "Dynamic analysis of partial-interactive composite beam with axial force", *J. Vib. Eng.*, **25**(5), 514-521.
- Wang, Y.C. (1998), "Deflection of steel-concrete composite beams with partial shear interaction", *J. Struct. Eng.*, **124**(10), 1159-1165.
- Wroblewski, T., Pelka-Sawenko, A., Abramowica, M. and Berczynski, S. (2012), "Modeling and analysis of free vibration of steel-concrete composite beams by finite element method", *Adv. Manuf. Sci. Technol.*, **36**(4), 85-96.
- Wu, Y.F., Xu, R.Q. and Chen, W.Q. (2007), "Free vibrations of the partial-interaction composite members with axial force", *J. Sound. Vib.*, **299**(4-5), 1074-1093.
- Xu, R.Q. and Wu, Y.F. (2007), "Static, dynamic, and bulking analysis of partial interaction composite members using Timoshenko's beam theory", *Int. J. Mech. Sci.*, **49**(10), 1139-1155.
- Zhang, S.B. (2014), "Experimental and theoretical study of dynamic properties for steel-concrete composite beam bridges with interlayer slip", Master Thesis; Southeast University, Nanjing, China. [In Chinese]

Zhou, W.B., Jiang, L.Z., Yu, Z.W. and Huang, Z. (2013), “Free vibration characteristics of steel-concrete composite continuous box girder considering shear lag and slip”, *Chia J. Highway Transport*, **26**(5), 88-94. [In Chinese]

CC

Appendix A

Solutions of Eq.(14)

Eq. (14) can be wrote as

$$\beta^2 \Lambda^3 - \alpha^2 \Lambda^2 - t^2 \Lambda + \alpha^2 t^2 = 0 \quad (\text{A1})$$

And comparing to the standard form of a cubic equation in one variable can be wrote as $ax^3 + bx^2 + cx + d = 0$, the real coefficients a, b, c and d in Eq. (A1) can be got

$$a = \beta^2, b = -\alpha^2, c = -t^2, d = \alpha^2 t^2 \quad (\text{A2})$$

In order to work out the Eq. (A1), three constants should be introduced

$$A = b^2 - 3ac = \alpha^4 + 3t^2 \beta^2 \quad (\text{A3})$$

$$B = bc - 9ad = t^2 \alpha^2 (1 - 9\beta^2) \quad (\text{A4})$$

$$C = c^2 - 3bd = t^2 (t^2 + 3\alpha^4) \quad (\text{A5})$$

And there is a discriminant Δ of Eq. (A1)

$$\Delta = B^2 - 4AC = \beta^4 \left(-\frac{12\alpha^8 t^2}{\beta^4} - \frac{12t^6}{\beta^2} - \frac{3\alpha^4 t^4}{\beta^4} - \frac{54\alpha^4 t^4}{\beta^2} + 81\alpha^4 t^4 \right) \quad (\text{A6})$$

In consideration of $\beta^2 < 1$, it is clear that

$$\frac{12\alpha^8 t^2}{\beta^4} + \frac{12t^6}{\beta^2} \geq 12 \times 2 \sqrt{\frac{\alpha^8 t^2}{\beta^4} \times \frac{t^6}{\beta^2}} = \frac{24\alpha^4 t^4}{\beta^3} > 24\alpha^4 t^4 \quad (\text{A7})$$

$$\frac{54\alpha^4 t^4}{\beta^2} > 54\alpha^4 t^4 \quad \text{and} \quad \frac{3\alpha^4 t^4}{\beta^4} > 3\alpha^4 t^4 \quad (\text{A8})$$

Substituting Eqs. (A7)-(A8) into Eq. (A6) produces

$$\Delta < 0 \quad (\text{A9})$$

It means that Eq. (A1) has three different real roots and one is negative while the other two are positive by using the relation of roots and coefficients a, b, c, d

$$\begin{cases} \Lambda_1 + \Lambda_2 + \Lambda_3 = \frac{\alpha^2}{\beta^2} > 0 \\ \Lambda_1\Lambda_2 + \Lambda_1\Lambda_3 + \Lambda_2\Lambda_3 = -\frac{t^2}{\beta^2} < 0 \\ \Lambda_1\Lambda_2\Lambda_3 = -\frac{\alpha^2 t^2}{\beta^2} < 0 \end{cases} \quad (\text{A10})$$

Going further, three roots can be obtained

$$\begin{aligned} \Lambda_1 &= \frac{-b - 2\sqrt{A} \cos \frac{\theta}{3}}{3a} = \frac{\alpha^2 - 2\sqrt{\alpha^4 + 3t^2\beta^2} \cos \frac{\theta}{3}}{3\beta^2} \\ \Lambda_2 &= \frac{-b + \sqrt{A}(\cos \frac{\theta}{3} + \sqrt{3} \sin \frac{\theta}{3})}{3a} = \frac{\alpha^2 + 2\sqrt{\alpha^4 + 3t^2\beta^2} \sin(\frac{\theta}{3} + \frac{\pi}{6})}{3\beta^2} \\ \Lambda_3 &= \frac{-b + \sqrt{A}(\cos \frac{\theta}{3} - \sqrt{3} \sin \frac{\theta}{3})}{3a} = \frac{\alpha^2 + 2\sqrt{\alpha^4 + 3t^2\beta^2} \sin(\frac{\theta}{3} + \frac{5\pi}{6})}{3\beta^2} \end{aligned} \quad (\text{A10})$$

where

$$\theta = \arccos T, \quad T = \frac{2Ab - 3aB}{2\sqrt{A^3}} = \frac{-2\alpha^6 - 9\alpha^2\beta^2t^2 + 27\alpha^2t^2\beta^4}{2\sqrt{(\alpha^4 + 3t^2\beta^2)^3}} \quad (\text{A10})$$

And $A > 0$, $-1 < T < 1$ must be met.

Appendix B

Solutions of constants c_i ($i = 1, 2, 3, 4, 5, 6$)

Considering the boundary conditions of simply supported beam

$$\Phi(0) = c_2 + c_4 + c_6 = 0 \quad (\text{B1})$$

$$\Phi^{(2)}(0) = -c_2\lambda_1^2 + c_4\lambda_2^2 + c_6\lambda_3^2 = 0 \quad (\text{B2})$$

$$\Phi^{(4)}(0) = c_2\lambda_1^4 + c_4\lambda_2^4 + c_6\lambda_3^4 = 0 \quad (\text{B3})$$

Eqs. (B1)-(B3) can be wrote as

$$\begin{bmatrix} 1 & 1 & 1 \\ -\lambda_1^2 & \lambda_2^2 & \lambda_3^2 \\ \lambda_1^4 & \lambda_2^4 & \lambda_3^4 \end{bmatrix} \begin{bmatrix} c_2 \\ c_4 \\ c_6 \end{bmatrix} = 0 \quad (\text{B4})$$

And the determinant of coefficient matrix

$$\begin{vmatrix} 1 & 1 & 1 \\ -\lambda_1^2 & \lambda_2^2 & \lambda_3^2 \\ \lambda_1^4 & \lambda_2^4 & \lambda_3^4 \end{vmatrix} = (\lambda_1^2 + \lambda_2^2)(\lambda_1^2 + \lambda_3^2)(\lambda_3^2 - \lambda_2^2) \neq 0 \quad (\text{B5})$$

In other words

$$c_2 = c_4 = c_6 = 0 \quad (\text{B6})$$

Meanwhile, another three equations can be got when considering the boundary conditions

$$\begin{aligned} \Phi(L) = c_1 \sin \lambda_1 L + c_3 \sinh \lambda_2 L + c_5 \sinh \lambda_3 L - \sum_{i=1}^N P_i \left[\frac{(\lambda_1^2 + \alpha^2) \sin \lambda_1 (L - x_i)}{\lambda_1 (\lambda_2^2 + \lambda_1^2) (\lambda_3^2 + \lambda_1^2)} \right. \\ \left. + \frac{(\lambda_2^2 - \alpha^2) \sinh \lambda_2 (L - x_i)}{\lambda_2 (\lambda_1^2 + \lambda_2^2) (\lambda_3^2 - \lambda_2^2)} + \frac{(\lambda_3^2 - \alpha^2) \sinh \lambda_3 (L - x_i)}{\lambda_3 (\lambda_1^2 + \lambda_3^2) (\lambda_2^2 - \lambda_3^2)} \right] = 0 \end{aligned} \quad (\text{B7})$$

$$\begin{aligned} \Phi^{(2)}(L) = -c_1 \lambda_1^2 \sin \lambda_1 L + c_3 \lambda_2^2 \sinh \lambda_2 L + c_5 \lambda_3^2 \sinh \lambda_3 L - \sum_{i=1}^n P_i \left[\frac{-\lambda_1^2 (\lambda_1^2 + \alpha^2) \sin \lambda_1 (L - x_i)}{\lambda_1 (\lambda_1^2 + \lambda_2^2) (\lambda_1^2 + \lambda_3^2)} \right. \\ \left. + \frac{\lambda_2^2 (\lambda_2^2 - \alpha^2) \sinh \lambda_2 (L - x_i)}{\lambda_2 (\lambda_1^2 + \lambda_2^2) (\lambda_3^2 - \lambda_2^2)} + \frac{\lambda_3^2 (\lambda_3^2 - \alpha^2) \sinh \lambda_3 (L - x_i)}{\lambda_3 (\lambda_1^2 + \lambda_3^2) (\lambda_2^2 - \lambda_3^2)} \right] = 0 \end{aligned} \quad (\text{B8})$$

$$\begin{aligned} \Phi^{(4)}(L) = & c_1 \lambda_1^4 \sin \lambda_1 L + c_3 \lambda_2^4 \sinh \lambda_2 L + c_5 \lambda_3^4 \sinh \lambda_3 L - \sum_{i=1}^n P_i \left[\frac{\lambda_1^4 (\lambda_1^2 + \alpha^2) \sin \lambda_1 (L - x_i)}{\lambda_1 (\lambda_2^2 + \lambda_1^2) (\lambda_3^2 + \lambda_1^2)} \right. \\ & \left. + \frac{\lambda_2^4 (\lambda_2^2 - \alpha^2) \sinh \lambda_2 (L - x_i)}{\lambda_2 (\lambda_1^2 + \lambda_2^2) (\lambda_3^2 - \lambda_2^2)} + \frac{\lambda_3^4 (\lambda_3^2 - \alpha^2) \sinh \lambda_3 (L - x_i)}{\lambda_3 (\lambda_1^2 + \lambda_3^2) (\lambda_2^2 - \lambda_3^2)} \right] = 0 \end{aligned} \quad (\text{B9})$$

The constants c_1, c_3, c_5 can be obtained from Eqs. (B7)-(B9)

$$c_1 = \sum_{i=1}^n P_i \frac{(\lambda_1^2 + \alpha^2) \sin \lambda_1 (L - x_i)}{\lambda_1 (\lambda_2^2 + \lambda_1^2) (\lambda_3^2 + \lambda_1^2) \sin \lambda_1 L} \quad (\text{B10})$$

$$c_3 = \sum_{i=1}^n P_i \frac{(\lambda_2^2 - \alpha^2) \sinh \lambda_2 (L - x_i)}{\lambda_2 (\lambda_1^2 + \lambda_2^2) (\lambda_3^2 - \lambda_2^2) \sinh \lambda_2 L} \quad (\text{B11})$$

$$c_5 = \sum_{i=1}^n P_i \frac{(\lambda_3^2 - \alpha^2) \sinh \lambda_3 (L - x_i)}{\lambda_3 (\lambda_1^2 + \lambda_3^2) (\lambda_2^2 - \lambda_3^2) \sinh \lambda_3 L} \quad (\text{B12})$$